Depinning Transitions in Interface Growth Models

Fábio D. A. Aarão Reis

Instituto de Física, Universidade Federal Fluminense,
Avenida Litorânea s/n, 24210-340 Niterói RJ, Brazil

Received on 16 April, 2003

Pinning-depinning transitions are roughening transitions separating a growing phase and pinned (or blocked) one, and are frequently connected to transitions into absorbing states. In this review, we discuss lattice growth models exhibiting this type of dynamic transition. Driven growth in media with impurities, the competition between deposition and desorption and deposition of poisoning species are some of the physical mechanisms responsible for the transitions, leading to different types of stochastic growth rules. The growth models are classified according to the those mechanisms and possible applications are shown, which include suggestions of experimental realizations of directed percolation transitions.

I Introduction

The study of surface and interface growth processes attracts much interest from the technological point of view mainly because it helps to understand the growth mechanisms of nanostructures and, consequently, their physical properties [1]. From the theoretical point of view, they motivated significant advances in non-equilibrium Statistical Mechanics and related fields [2, 3]. Theoretical modeling is usually based on stochastic differential equations or on discrete atomistic models. In various models, changing one parameter leads to a roughening transition between a rough and a smooth phase. Two well known examples are the transition in the Kardar-Parisi-Zhang equation in dimensions $d \geq 3$, separating regimes with linear (smooth) and nonlinear growth, and temperature-induced roughening transitions in equilibrium conditions [2]. On the other hand, in the so-called depinning transitions, the interface propagates only in the rough phase, being pinned in the smooth phase. Several mechanisms may be responsible for this type of transition, such as the presence of impurities in the growth media, competition between deposition and evaporation or formation of poisoning species at the growing surface. One of the interesting features of depinning transitions is that they frequently can be mapped onto transitions into absorbing states, whose most prominent example is directed percolation (DP). Different connections of depinning transitions to DP are found in discrete and continuous growth models, as well as connections with other classes of transitions to absorbing states [4] and, eventually, with statistical equilibrium transitions. Besides the fundamental interest of these systems, the large variety of interface growth phenomena observed in nature suggests them as strong candidates to experimental realizations of models of dynamic transitions, such as DP (see e. g. Ref. [5]).

The aim of the present work is to review the basic features of lattice growth models exhibiting depinning transitions. Before introducing these systems, we will briefly summarize the theory and phenomenology concerning interface growth and phase transitions into absorbing states (Sec. II). Then we will discuss the problem of growing interfaces in disordered media with quenched disorder, in which transitions in the DP class or in the class of the random field Ising model (RFIM) are the most frequently observed (Sec. III). We will be mainly interested in the problems of domain wall motion in the RFIM and directed percolation depinning, introduced in the works by Ji and Robbins [6], Tang and Leschhorn [8] and Buldyrev et al [7]. In those systems, the interface becomes pinned when the concentration of impurities is high enough to generate a blocking cluster running perpendicular to the growth direction. Subsequently, we will discuss a series of models with deposition and evaporation of weakly bonded atoms which were introduced by Alon et al [9] (Sec. IV). In these systems, the interface is pinned (but is not static) when evaporation rates are sufficiently high. Depending on the symmetries of the model, they show transitions in various classes, DP being one possibility. Finally, in Sec. V we will review some recent contributions of the present author, who analyzed models of deposition or etching with formation of poisoning species, showing different connections to DP transitions. Concluding remarks are presented in Sec. VI.

II Basic theory and phenomenology

A. Interface growth

Statistical growth models attract much attention because they describe real systems' features by representing the basic growth mechanisms as simple stochastic processes, neglecting the details of the microscopic interactions [2]. Some examples are the random deposition model with sur-

face relaxation of Family [10], the restricted solid-on-solid ($RSOS$) model of Kim and Kosterlitz [11] and the ballistic deposition (BD) model [12, 13]. These are called limited-mobility models because the diffusion of a deposited atom, whenever possible, takes place in a restricted time interval before the deposition of another atom. More complex models involve the competition among deposition, diffusion and aggregation [14, 15, 16], being able to represent real systems' features quantitatively.

During the growth process, the average height of the deposit, h, increases linearly in time, and the growth rate or growth velocity is given by

$$v = \frac{dh}{dt}. \tag{1}$$

In general, it is more interesting for the understanding of the growth dynamics to study the scaling of surface roughness. If deposition occurs in a d-dimensional lattice of length L, then we define the interface width at time t as

$$W(L,t) = \left[\left\langle \frac{1}{L^d} \sum_i \left(h_i - \overline{h} \right)^2 \right\rangle \right]^{1/2}, \tag{2}$$

which characterizes the global roughness of the surface. In this paper, we will usually refer to growth in $d+1$ dimensions instead of d, in order to avoid confusion with conventions of system dimensionality.

At early times, in the so-called growth regime, the interface width increases as

$$W \sim t^{\beta_G}, \tag{3}$$

where β_G is called the growth exponent. At long times, finite-size effects lead to width saturation at

$$W_{sat}(L) \equiv W(L, t \to \infty) \sim L^{\alpha_G}, \tag{4}$$

where α_G is called the roughness exponent. Here, the index G refers to growth, in order to distinguish these exponents from those of absorbing phase transitions. Fig. 1 illustrates the typical time behavior of the interface width.

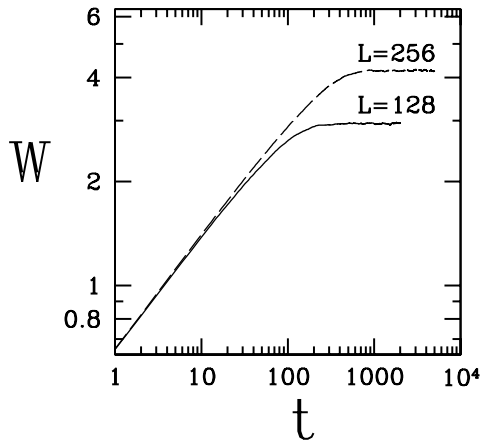

Figure 1. Interface width W versus time t for the RSOS model (Ref. [11]) in $1+1$ dimensions, in two different lattice lengths L.

Eqs. (3) and (4) are included in the dynamic scaling relation proposed by Family and Vicsek [13],

$$W = L^{\alpha_G} f\left(t L^{-z_G} \right), \tag{5}$$

where f is a scaling function and z_G is the dynamical exponent, given by

$$z_G = \frac{\alpha_G}{\beta_G}. \tag{6}$$

In Eq. (5), the argument of the scaling function is a ratio of the deposition time and the crossover (or saturation) time $\tau \sim L^z$. This crossover occurs when the lateral correlation length of the growth process, measured along the directions parallel to the surface, equals the lattice length L. In the direction normal to the surface, the correlation length is of the order of the interface width W.

The exponents α_G, β_G and z_G of the discrete models are expected to assume values predicted by related continuum theories, which represent those processes in the limits $L \to \infty$, $t \to \infty$, defining the universality classes of interface growth. The simplest theory for correlated growth was proposed by Edwards and Wilkinson [17], considering that the height distribution obeys certain symmetry requirements: translation, rotation and inversion symmetry in the directions parallel to the substrate, invariance under translation in time and translation along the growth direction, and reflection symmetry with respect to the mean height (up-down symmetry). These conditions lead to the Edwards-Wilkinson (EW) equation

$$\frac{\partial h}{\partial t} = \nu \nabla^2 h + \eta(\vec{x}, t), \tag{7}$$

where h is the height at the position $\vec{x}$ in a d-dimensional substrate at time t, ν represents a surface tension and η is a Gaussian noise with zero mean and variance $\langle \eta(\vec{x},t)\eta(\vec{x'},t') \rangle = D\delta^d(\vec{x}-\vec{x'})\delta(t-t')$. Higher order derivatives of h which satisfy the above symmetry requirements were not written in Eq. (7) because they are irrelevant under renormalization, not affecting the interface width exponents [2]. The dynamical exponent of the EW theory is $z_G = 2$ in any spatial dimension; in $d=1$, $\alpha_G = 1/2$ and $\beta_G = 1/4$, while in $d=2$, $\alpha_G = \beta_G = 0$, with logarithmic scaling in Eqs. (3) and (4) [2, 17].

The Family model [10] and the Wolf-Villain model [18] are two examples of discrete deposition models that belong to the EW class.

In many growth processes, the up-down symmetry is broken by some mechanism of lateral growth. Thus, nonlinear terms are included in the continuum growth equation, the more relevant one being proportional to $(\nabla h)^2$. Including this extra term in Eq. (7), we obtain the Kardar-Parisi-Zhang (KPZ) equation [19]

$$\frac{\partial h}{\partial t} = \nu \nabla^2 h + \frac{\lambda}{2} (\nabla h)^2 + \eta(\vec{x}, t), \tag{8}$$

where λ is called the excess velocity. Only in $d=1$ the KPZ exponents are exactly known: $\alpha_G = 1/2$, $\beta_G = 1/3$,

$z_G = 3/2$ [19]. In $d = 2$, which is the more relevant dimension for real applications, numerical works and renormalization studies give $\alpha_G \sim 0.4$ and $\beta_G \sim 0.25$ [2].

Several discrete models belong to the KPZ class, such as BD [12], the RSOS model [11] and a recently introduced etching model of Mello et al [20].

If the interest is MBE deposition, surface diffusion is an essential mechanism to describe interface width scaling. Its main effects led to the proposal of fourth order linear and nonlinear growth equations, which are reviewed in Refs. [2] and [3].

B. Phase transitions in systems with absorbing states

Here we will review the basic phenomenology of non-equilibrium phase transitions in models with absorbing states, i. e. configurations which can be reached by the dynamics but from which the system cannot leave. Good reviews on this topic and related subjects are in Refs. [4] and [21].

A simple model for the spreading of an infectious disease without immunization qualitatively illustrates this type of transition. Suppose that each individual of a population may be healthy or infected. A healthy individual may be infected upon contact with infected neighbors, while an infected one may recover from the disease. At long times, depending on the probabilities of contamination and recovery, the spreading process survives or the infection is completely eliminated. In the latter case, the system has evolved into an absorbing state, with no infected individual, and cannot leave that state. Related problems suitable for analytical solution are presented in Ref. [21].

One of the oldest lattice models showing a transition into an absorbing state is directed percolation [22] (DP), which was introduced as a variant of isotropic percolation [23, 24]. Fig. 2 illustrates the formation of clusters in cases of bond percolation, with the same fraction p of active lattice bonds. In isotropic percolation (Fig. 2a), starting from the central lattice site, a cluster is formed with all bonds that are connected to the center by a path of active bonds. Some isolated clusters of active bonds appear at the edges of the lattice. On the other hand, in DP, bond connectivity has a preferential direction, illustrated by arrows in Fig. 2b (down-right and down-left directions). Starting from the central site, the cluster of connected bonds is formed following the arrows. Thus, bonds which were present in the cluster of the isotropic problem are not present here, since a path with upwards movements would be necessary to reach them from that starting point.

The order parameter of both models is the probability P of a lattice site to belong to an infinite (percolating) cluster. For small values of p, we have $P = 0$, because only finite clusters are formed. As p increases, the average size of the clusters grow and, at a certain critical probability p_c, one infinite cluster appears. In two or more dimensions, the transition is continuous, with an increasing fraction of the lattice sites belonging to the infinite cluster for $p > p_c$. The critical behavior of P and other geometric quantities, such as correlation lengths, are very different in isotropic percolation and in DP.

DP in $d + 1$ dimensions ($1 + 1$ in Fig. 2b) may be interpreted as a dynamical process in a d-dimensional system, with time as the additional dimension [4]. The preferential direction of the lattice bonds (vertical in Fig. 2b) is the time direction. Another simple dynamical process with the main features of DP is the contact process [25] (CP), which was introduced as a lattice model for the spreading of an infection, as discussed above. One of the possible versions of the $1 + 1$-dimensional CP is the particle-hole problem illustrated in Fig. 3. An empty site at time t may be occupied by a particle at time $t + dt$ if it has at least one occupied neighbor. The rate of particle creation is $n\lambda/2$, where n is the number of neighboring particles. On the other hand, a particle may be annihilated with rate 1, independently of its neighborhood. Thus, the parameter λ, which represents the infection rate, plays the same role of the probability p in the DP problem. In $1 + 1$ dimensions, its critical value is $\lambda_c = 3.29785 \pm 0.00008$ [26]. The order parameter of the CP process is the occupied fraction ρ of the lattice, equivalent to the probability P in the DP model.

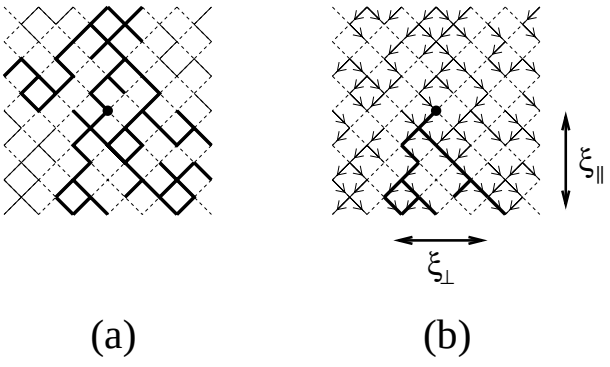

Figure 2. Illustration of (a) isotropic and (b) directed bond percolation in a two-dimensional lattice, with the connectivity in the DP problem restricted to the directions indicated by arrows. Solid lines represent active bonds and dashed lines represent inactive bonds, with the same (random) spatial distribution in both figures. Clusters generated from the central site are indicated by bold lines. The longitudinal and transversal correlation lengths in the DP problem are indicated.

The order parameters of these dynamical systems are obtained from configurational and time averages in their steady states. Near the critical points, they behave as

$$P \sim (p - p_c)^{\beta_T} \tag{9}$$

(similarly for ρ as a function of λ in the CP). Here, the index T refers to the dynamic transition, in order to distinguish this exponent from the growth exponent of interface width (Eq. 3). The CP and various other models have the same critical exponents of DP, thus belonging to the DP universality class. The best estimates of exponent β_T in $d = 1$ and $d = 2$ are $\beta_T = 0.276486 \pm 0.000008$ [27] and $\beta_T = 0.584 \pm 0.004$ [28], respectively.

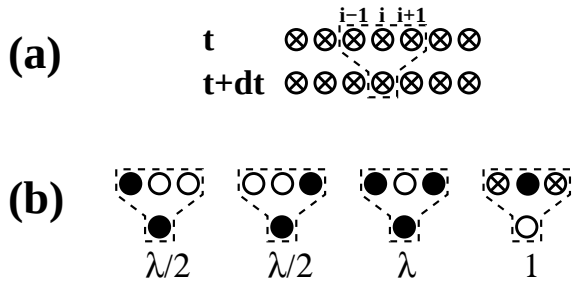

Figure 3. The contact process in $1+1$ dimensions, where full (empty) circles represent particles (holes) and crossed circles may represent a particle or a hole; (a) a scheme showing that the state of site i at time $t+dt$ depends on its state and on the state of its neighbors at time t; (b) the rates associated to creation and annihilation processes.

Other critical exponents describe the spatial and temporal correlations in these dynamical processes, whose characteristic lengths are illustrated in Fig. 2a. The longitudinal correlation length $\xi_{\|}$ of $d+1$-dimensional DP is a temporal length scale from the point of view of a dynamical process, characterizing the time correlations in this system. On the other hand, correlations along the d spatial dimensions are described by the transversal correlation length $\xi_{\perp}$. Near criticality, they behave as

$$\xi_{\|} \sim |p - p_c|^{\nu_{\|}} \tag{10}$$

and

$$\xi_{\perp} \sim |p - p_c|^{\nu_{\perp}}. \tag{11}$$

Usually, the critical exponents $\nu_{\|}$ and $\nu_{\perp}$ are very different. The best known estimates in $d = 1$ are $\nu_{\|} = 1.733847 \pm 0.000006$ and $\nu_{\perp} = 1.096854 \pm 0.000004$ [27], and in $d = 2$ they are $\nu_{\|} = 1.295 \pm 0.006$ and $\nu_{\perp} = 0.734 \pm 0.004$ [28]. No exact value of DP exponents in $d = 1$ and $d = 2$ is known yet.

One of the more interesting features of the DP class is that it includes systems defined with very different microscopic rules. Models with depinning transitions illustrate this fact, as will be shown in the next sections. Other important examples are forest-fire models [29] and models of catalytic reactions [30]. This observation led Janssen and Grassberger [31, 32] to conjecture that a model should belong to the DP class if it obeys the following conditions: 1) the model displays a continuous transition from a fluctuating active phase into a unique absorbing state; 2) the transition is characterized by a positive one-component order parameter; 3) the dynamical rules involve only short-range processes; 4) the system has no special attributes, such as additional symmetries or quenched randomness.

This conjecture has not yet been proved rigorously, but it is supported by a large amount of numerical results. Surprisingly, the DP class also includes some models which do not obey one of the above rules [4, 21]. The field-theoretical formulation of DP helps to understand the robustness of the DP class - see e.g. Ref. [4] and references therein.

There are also many non-equilibrium phase transitions into absorbing states that do not belong to the DP class. A class which deserves to be mentioned here is the parity conserving (PC) one, in which the simplest representative model is that of branching annihilating random walks with an even number of offspring [33]. This model is defined by the following reaction-diffusion scheme:

$$A \xrightarrow{\lambda} (n+1)A \qquad , \qquad 2A \xrightarrow{\alpha} 0, \tag{12}$$

where $n = 2, 4, 6, \ldots$ denotes the number of offspring and the reaction rates are indicated above the arrows. This dynamical process conserves the number of particles modulo 2. An absorbing transition is observed for all n with finite annihilation rates α. In $1+1$ dimensions, the best known estimates of critical exponents for the PC class are $\beta_T = 0.92 \pm 0.02$, $\nu_{\|} = 3.22 \pm 0.06$ and $\nu_{\perp} = 1.83 \pm 0.03$ [34].

III Growing interfaces in disordered media

In Fig. 4, we show a schematic representation of the problem of an interface in a disordered medium driven by an external force of modulus F. The disorder acts as an inhomogeneous friction force which pins some parts of the interface. For small values of F, the interface moves in the direction of the force but will eventually become pinned by the impurities. The interface is depinned with a critical driving force F_c. Near and above this critical value, the growth velocity scales as

$$v \sim (F - F_c)^{\theta}, \tag{13}$$

where θ is called the velocity exponent. This exponent and the interface width exponents of the critical interface characterize the universality class of the depinning transition.

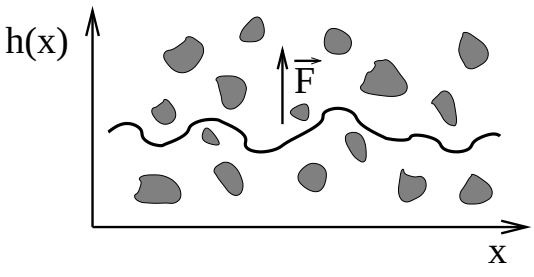

Figure 4. Schematic representation of a driven interface in a disordered media.

Several lattice growth models represent the generic problem of an interface moving in a disordered medium.

They are usually separated in two groups, depending on the effects of anisotropy at the transition points. The first group is that of isotropic growth models, whose main representative is the problem of domain wall motion in the random-field Ising model [6, 35, 36] (RFIM), and the second one includes models of directed percolation depinning (DPD) [7, 8]. The common ingredient of these models is the presence of quenched disorder, which eventually form spanning clusters that block an interface growth.

The different universality classes are related to the presence of nonlinear terms in the expected hydrodynamic description of the interface at criticality. The most general equation is the quenched KPZ (QKPZ) equation

$$\frac{\partial h}{\partial t} = F + \nu\nabla^2 h + \frac{\lambda}{2}(\nabla h)^2 + \eta(\vec{x}, h), \qquad (14)$$

where the thermal noise $\eta(\vec{x}, t)$ of the KPZ equation (8) is replaced by a quenched noise $\eta(\vec{x}, h)$ [37, 38, 39]. Here, the main idea is that, at criticality, this quenched noise dominates the depinning process over the thermal noise. While the models in the DPD class show finite (possibly infinite) coefficients λ of the nonlinear term at criticality, the models in the RFIM class, in the self-affine regimes, have vanishing nonlinear terms. Eq. (14) in the case $\lambda = 0$ is called quenched EW (QEW) equation. These distinct critical behaviors reflect the symmetries of the underlying media [40].

Before going further into the discussion of continuum theories, we will introduce the main lattice models.

First we consider depinning transitions in the RFIM. In this problem, spins with possible values $s_i = \pm 1$ at sites i of a lattice interact through the Hamiltonian

$$\mathcal{H} \equiv -J \sum_{\langle i,j \rangle} s_i s_j - \sum_i (h_i + H)\, s_i, \qquad (15)$$

where the first sum is over pairs of nearest neighbors, J is a ferromagnetic coupling, H is an external uniform field and h_i is a quenched local field which represents the disorder in this system. In the simplest version of the model, $J = 1$ (fixed) and h_i is randomly distributed in the interval $[-\Delta, \Delta]$. Thus, Δ characterizes the strength of the disorder and H plays the role of the driving force.

The dynamics of an interface separating domains of $+1$ and -1 spins is usually simulated at zero temperature, starting from a flat interface, with up $(+1)$ spins above it and down (-1) spins below it. For simplicity, $H \geq 0$ is considered. The interface advances by flipping down spins adjacent to the interface if it lowers the energy of the system. Regions of down spins which become surrounded with up spins become trapped in that state. Parallel or random updates may be considered [35].

For small values of H, the stable phase of $+1$ spins begins to advance at the expense of the -1 phase. However, the system will eventually attain a static configuration, in which -1 spins at the interface are frozen by random local fields h_i favoring this configuration. For a critical field $H = H_c$ (a function of Δ), the interface becomes depinned, and moves with finite velocity for $H > H_c$.

In the $1+1$-dimensional RFIM, two different morphologies may be observed in the critical region: for $\Delta < 1.0$, the interface is faceted, while for $\Delta > 1$ it is self-similar. A schematic representation of the phase diagram is shown in Fig. 5. In the self-similar regime ($\Delta > 1$), the interface problem cannot be represented by the QEW equation (Eq. 14 with $\lambda = 0$), but can be mapped onto site percolation. The local field $H + h_i$ alone determines the stability of spin s_i, then all spins with high enough local fields will eventually be flipped, while the other spins block the growth. At criticality, a critical percolation cluster of -1 spins blocks the growth, the interface being the perimeter of this cluster [35, 36]. Consequently, the critical interface is self-similar, with roughness exponent $\alpha_G = 1$. Scaling arguments [35] give the velocity exponent $\theta = \nu\,(d_{min} + 1 - d_F)$, where ν is the correlation length exponent of the percolation problem, d_F is the fractal dimension of the critical percolation cluster and d_{min} is the dimension of the shortest paths along that cluster [24].

In $2 + 1$ dimensions, the RFIM shows a transition line in the (Δ, H) diagram with a faceted region, a self-similar region and a self-affine region. In this self-affine region, numerical results suggest that the critical interfaces can be represented by the QEW equation. Among these results are the measure of growth velocities of tilted interfaces and of critical roughness exponents [41].

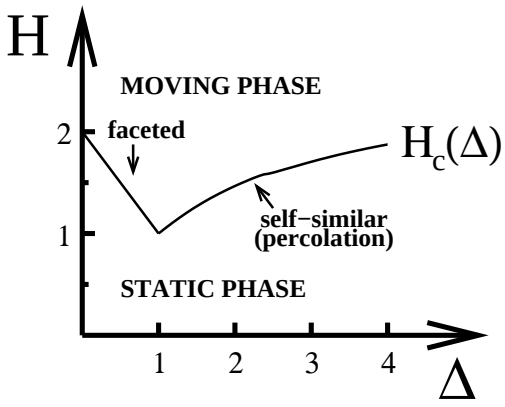

Figure 5. Schematic representation of the phase diagram of the random-field Ising model in $1 + 1$ dimensions, where H is the external field and Δ is an amplitude of random local fields.

Experiments on fluid flow in porous media are possible realizations of the isotropic class [42, 43, 44]. The former estimates of roughness exponents were scattered in the range $0.65 - 0.91$. However, some recently developed methods were applied to analyze theoretical and experimental data and showed that fluid flow in random media formed by packed glass beads were indeed in the RFIM class [45].

Now we will discuss the anisotropic class of depinning transitions, whose main representatives are the DPD model of Buldyrev et al [7] and a related model by Tang and Leschhorn [8]. The DPD model was introduced to describe

results of experiments on paper wetting. Fig. 6a illustrates the process on a square lattice with a fraction p of blocked sites and a fraction $1-p$ of empty sites. At $t=0$ the interface is flat (all heights $h=0$), with all sites below it being wet. Growth proceeds as follows: first, an empty site which is a nearest neighbor of the interface is chosen; then, this site is wet and any other site below it (same x, lower h) is also wet, independently of being empty or blocked. Thus, the model excludes overhangs.

For small p, the interface advances with finite velocity. The fraction $1-p$ of empty sites plays the role of the driving force in this model. When p attains a sufficiently large value that a DP cluster is formed in the x direction (perpendicular to the growth direction), the interface becomes pinned. Fig. 6b illustrates the formation of such cluster and the resulting pinned interface. The condition of wetting a whole column justifies the requirement of a DP cluster to stop the growth, since an isotropic percolation cluster would be crossed by the wetting process at the overhangs. Consequently, the depinning transition occurs at the DP threshold $p=p_c\approx 0.469$ of this geometry (connectivity of blocked cells through next nearest neighbors in the square lattice is assumed - see Fig. 6b).

The mapping of this transition onto DP is possible only in $1+1$ dimensions. In higher dimensions, the transition can be mapped onto the problem of percolation of directed surfaces [47].

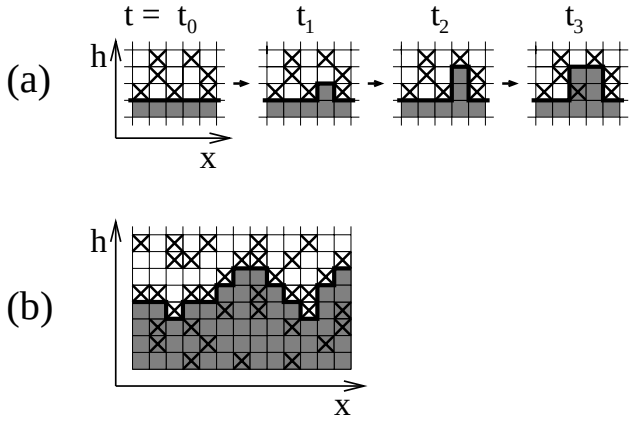

Figure 6. (a) The directed percolation depinning model, with empty squares, crossed squares and filled squares representing empty cells, blocked cells and wet cells, respectively. At time t_0, the interface (heavy line) is flat. At $t=t_1$ and $t=t_2$, one empty cell which has a neighboring wet cell is wet. At $t=t_3$, an empty cell neighboring the interface is wet, and the blocked cell below it is also wet. (b) Pinned interface due to the presence of a directed percolating cluster of blocked cells above it, running along the x direction.

Scaling arguments in $1+1$ dimensions give a velocity exponent $\theta=\nu_\parallel-\nu_\perp\approx 0.637$ and a roughness exponent $\alpha_G=\nu_\perp/\nu_\parallel\approx 0.633$ at criticality [7, 8]. These relations are supported by numerical estimates of the exponents θ and α_G of the DPD and related models [7, 8, 41].

The first estimate of the roughness exponent in experiments on paper wetting were in good agreement with the above theoretical prediction [7], but other authors' experiments provided larger values of α_G [46]. Since it was only a ratio of exponents that agreed with DP values, it was not clear whether they were indeed experimental realizations of DP. However, experiments on ink flow in a sponge-like material gave roughness exponents consistent with the extension of the DPD model to $2+1$ dimensions [47] (which is not in the DP class), which suggests further experimental studies on these lines.

The above analysis illustrates the fact that the DPD and related models belong to a class of anisotropic depinning. On a phenomenological level, it is believed that the QKPZ equation (14) provides their continuum description at criticality [40, 41], with anisotropy being responsible for the presence of a non-vanishing nonlinear term. It contrasts to the usual kinetic origin of nonlinearities in the growth equations ($\lambda\sim v$) [19], which would give $\lambda=0$ at the transition. That belief is supported by calculations of the growth velocities of tilted interfaces, which indicate a non-vanishing (possibly infinite) nonlinear term [41]. The same analysis indicates that some models, such as the RFIM in $2+1$ dimensions (self-affine regime), correspond to the QEW class.

Despite the intense study of this subject in the last ten years, there are some open questions that motivate further analysis of the QKPZ equation, its connection to directed percolation depinning and related topics. See, for instance, the recent works of Neshkov [48], Ramasco et al [49] and Le Doussal and Wiese [50].

IV Competitive models with deposition and evaporation

Depinning transitions are also observed in systems with deposition and evaporation of atoms. In some cases, evaporation is restricted to the edges of islands, and the transitions can be mapped onto DP and other absorbing state transitions. Physically, these processes account for the lower binding energies of adatoms which are isolated above an island or aggregated at its border, when compared to the energy inside an island. Extended models may also include evaporation inside the islands, leading to more complicated critical behavior.

Fig. 7a shows the growth rules of the first model proposed with those features [9], in $1+1$ dimensions. Atoms are deposited with probability q. Evaporation occurs with probability $1-q$ for isolated atoms (no lateral neighbor) and with probability $(1-q)/2$ for atoms with one lateral neighbor, i. e. atoms at the edge of an island. These processes must also obey the condition of the RSOS model [11] that $|h_x-h_{x\pm1}|\leq 1$, otherwise the deposition or evaporation attempt is rejected. No evaporation occurs below the bottom layer.

For small q, evaporation processes dominate, then the interface is pinned to the bottom layer. As q increases, larger and higher islands are formed. If any region of the bottom layer is not filled, evaporation of the whole deposit is still possible and the average height is limited, characterizing the pinned phase. The depinning transition takes place when

the bottom layer is completely filled, because no evaporation can occur at that layer anymore. Subsequently, higher layers will also become completely filled. The critical evaporation probability obtained in simulations is $q_c \approx 0.189$ [9].

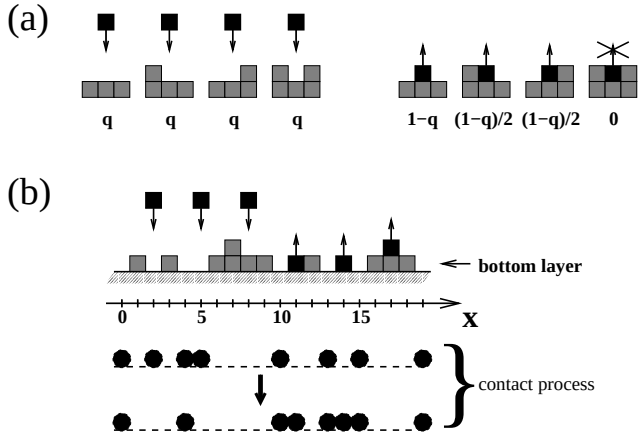

Figure 7. (a) Conditions for deposition and evaporation of particles in the model with evaporation restricted to the edges of the islands, with the respective probabilities. (b) Above the x axis, some deposition and evaporation attempts in the interface problem are shown. Below the axis, the configurations of the associated particle-hole problem before and after the deposition and evaporation processes are shown.

This transition can be mapped onto a CP by associating a particle-hole problem to the dynamics at the bottom layer. In this problem, a particle corresponds to an empty column of the deposit ($h = 0$), while a hole corresponds to a filled column ($h > 0$). Some deposition and evaporation attempts and the corresponding configurations of the particle-hole system (before and after those processes) are shown in Fig. 7b. The annihilation process (particle $\rightarrow$ hole) of the CP corresponds to the deposition of an atom at an empty column. Offspring production (hole $\rightarrow$ particle) corresponds to the evaporation of an atom at the bottom layer. This is possible only if that atom has an empty neighbor in the interface problem (Fig. 7a), which corresponds to a neighboring particle in the particle-hole system. The rates of annihilation and offspring production cannot be obtained analytically from q because the deposition and evaporation processes must obey the RSOS condition and, consequently, those rates depend on the heights distribution. However, for an unrestricted model, the exact mapping on a CP is possible, with the annihilation rate given by $\lambda = q/(1-q)$ [51].

This analysis shows that this depinning transition is also in the DP class, with the smooth phase (rough phase) corresponding to the active phase (absorbing phase) of DP. However, there is an important difference from the problems of interfaces growing in disordered media: in the pinned phase, the deposit dynamically evolves through different configurations, i.e. it is not blocked.

The scaling of the interface velocity is obtained as follows. For q slightly above q_c, a large time Δt is necessary to fill the bottom layer. This is the characteristic time of survival of isolated empty sites at the bottom layer, which correspond to particles in the CP. Thus, $\Delta t \sim \xi_{\parallel}$. Since this is the typical time for filling one layer ($\Delta h \approx 1$), we obtain

$$v \sim \frac{\Delta h}{\Delta t} \sim {\xi_{\parallel}}^{-1} \sim (q - q_c)^{\nu_{\parallel}}. \qquad (16)$$

The bottom layer occupation n_0 in the smooth phase corresponds to the fraction of particles in the corresponding particle-hole problem, then its critical behavior obeys

$$n_0 \sim (q_c - q)^{\beta_T}, \qquad (17)$$

with the DP exponent β_T. On the other hand, finite-size scaling relations of various quantities involve the lateral correlation exponent $\nu_{\perp}$ of DP [51]. These relations and the scaling forms in Eqs. (16) and (17) are confirmed by numerical simulations of the model [9, 51].

The interface width at the smooth phase saturates, while at the rough phase it scales with KPZ exponents [51]. At criticality, it was recently shown [52] that, in lattices of length L, W obeys the finite-size scaling relation

$$W^2(L,t) = a \ln L + f\left(t/L_c^z\right), \qquad (18)$$

where a is a constant and f is a scaling function. In Eq. (18), the critical dynamical exponent is given by $z_c = \nu_{\parallel}/\nu_{\perp}$ [51], and logarithmic scaling means $\beta_G = \alpha_G = 0$ at criticality.

Another interesting feature of this depinning transition is the scaling of the occupations n_k of the first few layers ($k = 1, 2, \ldots$), which is connected to unidirectionally coupled DP processes. Numerical simulations and field-theoretical renormalization techniques were applied to this problem [51, 53]. One important conclusion is that the scaling exponents ${\nu_{\parallel}}^{(k)}$ and ${\nu_{\perp}}^{(k)}$ of the dynamical processes at higher layers are the same of DP [51], although the critical behavior of n_k (analogous to Eq. 17) is governed by k-dependent exponents.

Concerning possible experimental realizations of this transition, the main limitation is the exclusion of adatom diffusion in the model, which typically occurs with much higher rates than desorption.

A related model was proposed by Hinrichsen and collaborators to describe non-equilibrium wetting transitions [54]. Deposition and evaporation at the edges of plateaus may occur with probabilities proportional to q and 1, respectively. Moreover, evaporation inside an island is also possible, with probability proportional to p (the last process in Fig. 7a). The presence of a hard wall is considered at $h = 0$, representing a solid substrate. For $p = 0$, we have the previous model, in which a complete layer is stable and a DP transition is observed. The case $p = 1$ can be solved exactly because the probabilities of evaporation are equal at all positions and, consequently, the dynamic rules satisfy detailed balance [54]. The critical interface at $(p = 1, q = 1)$ is in the EW class. However, in the generic case $0 < p < 1$ the situation is less clear: the model is expected to be described by a KPZ equation with an additional term for the effective interaction between the hard wall and the interface [55, 56], but the theoretical exponents significantly differ from numerical estimates. This divergence was attributed to a crossover between the values predicted by this continuum theory and the exact exponents at $p = 1$. For details, see Refs. [4] (Sec.

6.7), [54] and [57], the latter presenting an extended wetting model.

Another interesting model is that of dimer deposition and desorption in which desorption is allowed only at the edges of the plateaus, similarly to the model in Fig. 7 [58]. Fig. 8a illustrates the growth rules of the dimer model, with probability q for deposition and $1-q$ for desorption, respecting the RSOS condition. Moreover, both atoms of the pair must be at the same layer to aggregate or to evaporate. Consequently, the number of particles at each layer is conserved modulo 2.

A depinning transition is observed at $q_c \approx 0.317$. The dynamics at the bottom layer corresponds to a particle-hole problem with parity conservation, illustrated in Fig. 8b. Dimer deposition corresponds to pair annihilation and dimer desorption (possible only with an empty neighbor at the bottom level) corresponds to creation of a pair from one particle. A mapping onto a BAWE (Eq. 12) is possible, so that the transition belongs to the PC class (Sec. II.A). Numerical results confirm this hypothesis [58].

At criticality, the interface width and the average height increase as $W^2 \sim \langle h \rangle \sim \log t$. One curious feature of this model is that, in the depinned phase, the average height and the interface width also increase logarithmically, as $\langle h \rangle \sim W \sim \log t$, i. e. the interface does not move with a constant velocity. This is related to the fact that random deposition of dimers does fill a line completely, but leaves isolated holes between islands, in which new dimers cannot be deposited. In Fig. 8b, this is the case at $x = 6$ after deposition and at $x = 15$ before desorption. In the interface model, it leads to the formation of mounds, with the one-site valleys between them acting as pinning centers. In order to deposit a new dimer, it is necessary that two pinning centers diffuse until they meet. However, this diffusion is very slow because it depends on the evaporation of entire mounds in a phase where deposition is dominant.

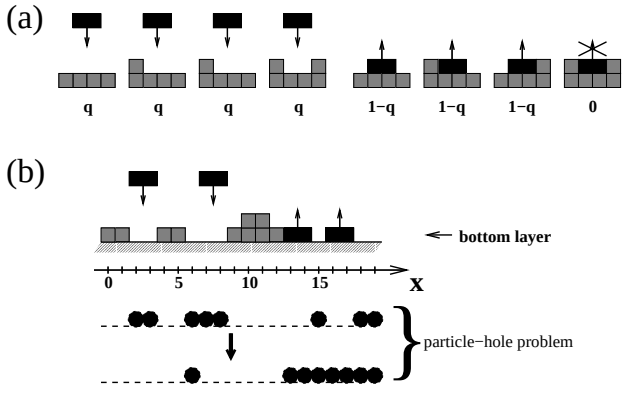

Figure 8. (a) Conditions for dimer deposition and evaporation in the model with evaporation restricted to the edges of the islands, with the respective probabilities. (b) Above the x axis, some deposition and evaporation attempts in the dimer deposition problem are shown. Below the axis, the configurations of the associated particle-hole problem before and after the deposition and evaporation processes are shown.

For a more detailed review on the problems discussed in this Section and related models, the interested reader may consult Ref. [4] and references therein.

V Growth with poisoning species

In 1983, Wang and Cerdeira [59] introduced a class of deposition models with two kinds of incident particles, A and B, and with production of an inactive species C after reactions between an incident B and an aggregated A. Some years later, works on $2+1$-dimensional versions of this model and its extensions suggested the existence of a morphological transition for high fluxes of particles B [60, 61] (the nature of this transition was not analyzed there). Motivated by these works and by some experiments mentioned below, related (and apparently different) models were recently considered. They involve the competitive deposition of a main species and a poisoning one, showing depinning transitions as the relative fluxes are varied [62, 63]. The most interesting cases are those with transitions in the DP class, which will be the central point of discussion in this section.

In the following models, we will denote the active species by A and the poisoning species by B. An A particle is released with probability $1-p$ and a B particle is released with probability p above the deposit. The role of species B is to block the surface for future aggregation of any incident particle at its neighborhood.

The most simple transition occurs in a RSOS version [62] of the original AC model [59]. Its rules are illustrated in Fig. 9. Any incident particle can aggregate at the top of the column of incidence only if: 1) it has a neighboring A at that position; 2) the aggregation respects the condition that heights differences of neighboring columns do not exceed 1 [11]. In the RSOS model ($p = 0$) the interface grows with finite velocity. A first order dynamic transition is observed at $p = 0$ because any small flux of B leads to the formation of pinning centers that will eventually block the growth process. A region of a blocked deposit for $p = 0.1$ is shown in Fig. 10a, while Fig. 10b shows the structure of the most probable pinning centers. No deposition occurs at valleys with those triplets of particles B due to condition 1 above, while no deposition occurs at the sloped regions of the surface due to condition 2. In the blocked phase, scaling arguments show that the interface width and the average height saturate as $W_s \sim H_s \sim p^{-3/2}$, which agrees with numerical results [62].

Subsequently, a ballistic-like model with similar aggregation rules was considered [63]. Fig. 11a illustrates its rules in $1+1$ dimensions. The incident particle (A or B) follows a straight vertical trajectory towards the surface. Aggregation is allowed only if the incident particle encounters a particle A at the top of the column of incidence or at the top of a higher neighboring column. Otherwise the aggregation attempt is rejected. A column in which aggregation (top or lateral) is possible is called an active column. The deposition time is the number of deposition attempts per substrate

column, thus the growth velocity (or growth rate) is equal to the fraction ρ of active columns.

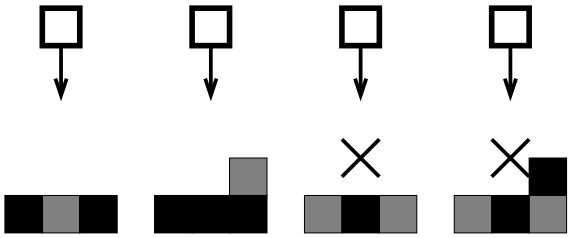

Figure 9. Examples of applications of the growth rules of the model with active (gray squares) and poisoning (black squares) particles, and the RSOS condition for aggregation.

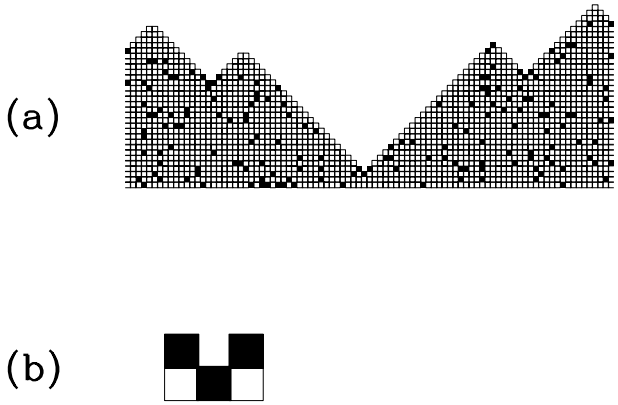

Figure 10. (a) A region of a blocked deposit in the model with poisoning species and RSOS condition for aggregation, for $p = 0.1$. (b) Structure of a triplet that blocks the growth at the valleys of the deposit.

As the flux of species B increases, the growth velocity decreases, and a pinning transition is observed at $p_c \approx 0.207$ in $1+1$ dimensions and $p_c \approx 0.490$ in $2+1$ dimensions [63]. The relation to DP is explained by the mapping of the interface problem in $d+1$ dimensions onto a d-dimensional CP. In the particle-hole problem, a particle is associated to a top A and a hole is associated to a top B, as shown in Fig. 11b. Note that this correspondence is the inverse of that considered in the problems of deposition and desorption in Sec. IV. Here, the deposition of a B in a column with a top A corresponds to the annihilation of a particle in the CP. On the other hand, the deposition of an A in a column with a top B corresponds to offspring production in the CP, since it requires a top A at a neighboring column. The stability of the absorbing state is illustrated by process 4 in Fig. 11b. The probabilities of annihilation and offspring production in the CP are not trivially related to p because they also depend on the heights' distribution.

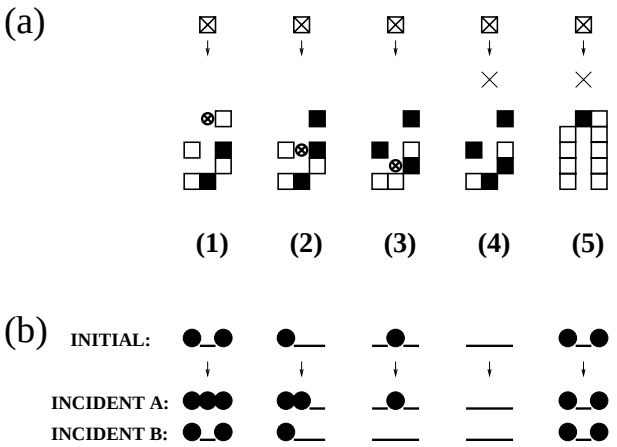

Figure 11. Ballistic-like deposition with a poisoning species. (a) Examples of deposition attempts in $d = 1$. Open squares represent particles A, filled squares represent particles B and crossed squares represent incident particles (A or B). In processes (1), (2) and (3), aggregation occurs at the positions marked with a crossed circle. In processes (4) and (5) the aggregation attempt is rejected. In processes (3) and (4), lateral aggregation to the right is not possible because the neighboring A is not at the top of its column. (b) The equivalent one-dimensional contact process, in which a top A corresponds to a particle (filled circles) and a top B corresponds to a hole (empty sites). The initial configuration and the possible final configurations, for the cases of incident A and incident B, are shown.

The growth phase ($p < p_c$) of this model corresponds to the active phase of the CP or DP. This correspondence is the opposite in all depinning transitions previously discussed: in growth in disordered media, depinning is observed if the impurities do not form a directed percolating cluster, and in the deposition-desorption models depinning occurs with a filled bottom layer, corresponding to absorbing phases of certain dynamic processes at that layer.

In an infinite lattice, a steady state with a fluctuating finite fraction of active columns is attained. Thus, the growth velocity is the order parameter of this transition and scales as

$$v \sim \epsilon^{\beta_T} \qquad , \qquad \epsilon \equiv p_c - p. \tag{19}$$

Here, the velocity exponent θ, in the language of driven interfaces, is equal to the order parameter exponent β_T of DP. At the transition point, the growth velocity is expected to decrease as $v_c \sim t^{-\beta_T/\nu_\parallel}$. These scaling relations are supported by numerical results [63].

At criticality, the fraction of growing columns is finite, decreasing in time as a power law. Consequently, there is a slowly increasing fraction of blocked columns. A region of a critical deposit in $1+1$ dimensions is shown in Fig. 12. The heights' differences between blocked and active columns increase linearly in time, then the interface width W is also expected to increase linearly in time, which is confirmed by numerical simulations [63]. On the other hand, at the growth phase, W asymptotically obeys KPZ scaling. Thus, below but near p_c, a crossover from a critical DP behavior ($W \sim t$) to KPZ scaling (Eq. 3) is observed, as shown in Fig. 13. The crossover time is of the order of the longitudinal correlation length of DP (Eq. 10).

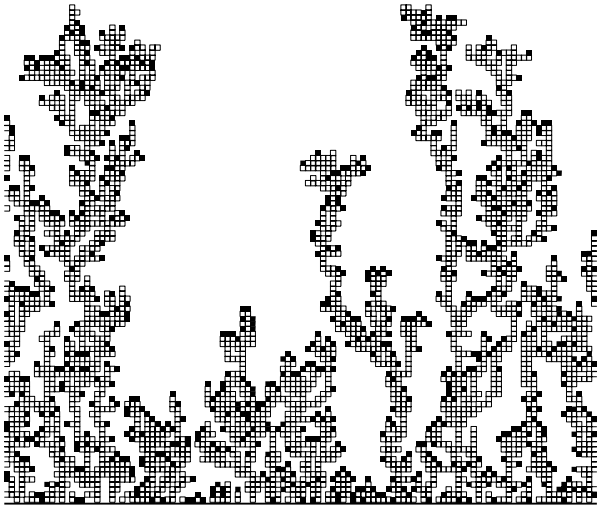

Figure 12. Critical deposit in $1+1$ dimensions for the ballistic-like model with a poisoning species. Open squares represent active particles and filled squares represent poisoning particles.

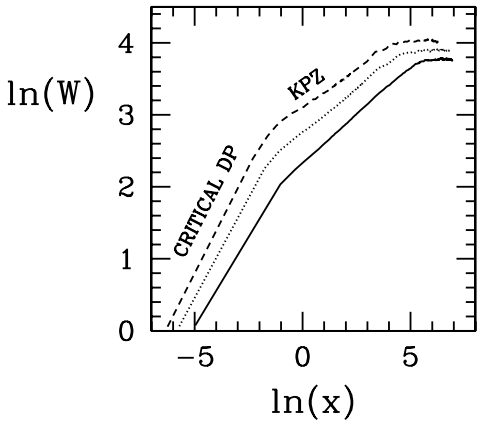

Figure 13. Interface width scaling in the ballistic-like model with a poisoning species below the critical point. Shown is $\ln W$ versus $\ln x$, with the scaling variable $x \equiv t\epsilon^{\nu_\parallel}$, for $p = 0.15$ (solid line), $p = 0.17$ (dotted line) and $p = 0.18$ (dashed line), in a lattice with length $L = 4096$. The regions of critical DP and KPZ behaviors are indicated.

Similar crossover was observed in the study of dynamical phase transitions in the Domany-Kinzel cellular automata by de Sales et al [64]. Those authors calculated the transition points with accuracy by mapping cellular automata patterns onto an interface problem, which showed a crossover from random deposition behavior ($\beta_G = 1/2$) to critical DP behavior ($\beta_G = 1$).

In the pinned (or blocked) phase, the deposit grows until attaining a limiting average height H_s, where the whole surface is poisoned by species B. Since surface poisoning corresponds to the absorbing phase in the CP, H_s is of the order of the longitudinal correlation length $\xi_\parallel$ of DP, which also agrees with numerical results [63]. The interface width of the blocked deposits also scales as $\xi_\parallel$.

Another interesting feature of this model (not discussed in Ref. [63]) is that the critical roughness exponent α_G is larger than one, i. e. it exhibits super-roughening [65]. Consider growth in finite lattices at the critical probability p_c, so that a finite fraction of the deposits will attain the steady state regime. At certain probability $p < p_c$, the transversal DP correlation length equals the lattice length, i. e. $\xi_\perp \sim \epsilon^{-\nu_\perp} \sim L$, and saturates at this value in the whole critical region, as expected from finite-size scaling theory [66, 67]. On the other hand, height fluctuations saturate at a value of the order of the longitudinal DP correlation length, then $W \sim \epsilon^{-\nu_\parallel}$. Thus, the saturation widths (Eq. 4) at the critical point scale with a roughness exponent

$$\alpha_G^{(c)} = \nu_\parallel / \nu_\perp . \tag{20}$$

This relation was confirmed numerically in $1+1$ dimensions. In Fig. 14a we show $W_{sat}\,(L)$ versus L at criticality ($128 \leq L \leq 4096$), and in Fig. 14b we show the effective exponents $\alpha_G^{(c)}\,(L)$ (local declivities of the previous log-log plot), which suggests an asymptotic exponent $\alpha_G^{(c)} \sim 1.6$. On the other hand, the best known estimates of DP exponents give $\nu_\parallel/\nu_\perp \approx 1.581$ [27].

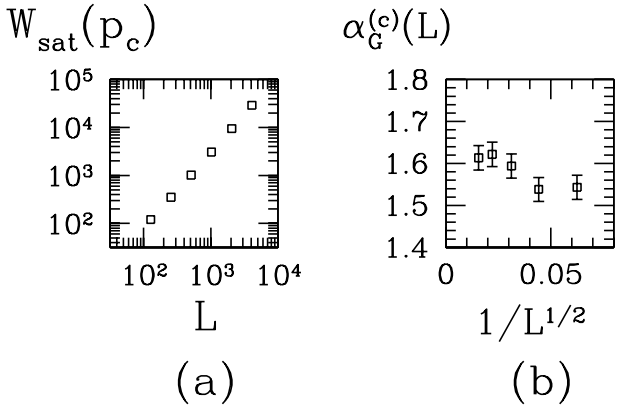

Figure 14. Interface width scaling in the ballistic-like model with a poisoning species at the critical point: (a) saturation width versus lattice length L at the critical point in $1+1$ dimensions, for $128 \leq L \leq 4096$; (b) effective roughness exponents (successive declivities of the data in (a)) versus $1/L^{1/2}$. This abscissa was chosen to clarify the evolution of the data with L.

Although the applicability of this ballistic-like model to real deposition processes is very limited, the robustness of the DP class suggests that systems with deposition of poisoning species but different aggregation mechanisms may also present transitions in that class. In various processes, the presence of different chemical species improves films' properties but leads to undesired features, such as the decrease of growth rates. In many cases, a poisoning species is responsible for the saturation of dangling bonds at the surface, such as deposition of Si films doped with P by CVD or MBE, in atmospheres with phosphine [68, 69]. Poisoning effects also appear in diamond CVD in atmospheres with boron and nitrogen [70], where high fluxes of boron cancel out diamond growth, leading to a transition to a blocked or pinned phase.

A related model was recently proposed for etching of a crystalline solid with deposition of a poisoning species after

reactions at the surface [71]. The lattice model without impurities ($p = 0$) was proposed in Ref. [20]. At each etching attempt, a random column i is chosen and the top particle is removed. Then, any neighboring column whose height is larger than the previous height of column i ($h_0(i)$) is etched until its own height becomes $h_0(i)$. These processes will be called normal and lateral erosion, respectively. Lateral erosion accounts for the removal of highly exposed parts of the solid after a normal erosion process. The rules of the extended model with a poisoning species are illustrated in Fig. 15. The solid contains a single chemical species A, similarly to the original model, and any column with a top A is said to be exposed. An erosion process (normal or lateral) at a certain column may leave an inactive particle B at the top of this column with probability p. Any attempt of normal erosion at a column with a top A (B) is accepted (rejected), then species B blocks the interface for this process. However, a column with a top B will be subject to lateral erosion if: 1) a neighboring column was subject to normal erosion; 2) there is an exposed particle A below the top B. This is the case of column $i = 7$ in Fig. 15.

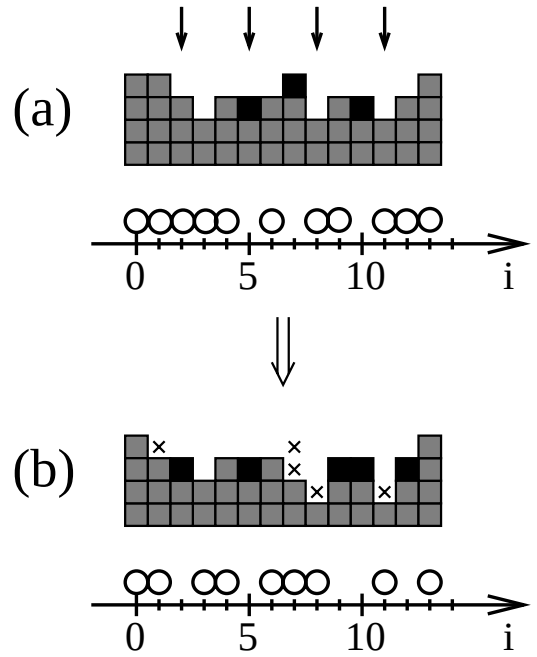

Figure 15. Etching model with a poisoning species: (a) examples of etching attempts in $d = 1$, with selected columns indicated by arrows, A particles in gray and B particles in black. The corresponding configuration of the associated one-dimensional particle-hole problem is shown below the solid, with particles (circles) corresponding to top A and holes corresponding to top B. (b) The solid after the etching attempts in (a), with positions of removed atoms indicated by crosses. Normal erosion at column 2 and lateral erosion at columns 9 and 12 left B particles at those columns. In column 7, a B particle was removed by lateral erosion. The configuration of the associated particle-hole problem is also shown.

It is also possible map this model onto a CP. A column of the solid with a top A is associated to a particle in a d-dimensional lattice, while a column with a top B is associated to a hole. This relation is also illustrated in Fig. 15. Normal and lateral erosion in the etching model give rise to particle annihilation and offspring production in this particle-hole system. Since lateral etching may occur at two ($d = 1$) or more ($d > 1$) columns, two or more offspring may be produced. Moreover, this CP also includes particle diffusion [71]. However, these features are not sufficient to change the class of the transition, which is confirmed to be DP by numerical simulations [71].

One of the motivations for this etching model is the fact that, in some experiments, deposition of poisoning species is observed. One example is Si etching by $NaOH$, where some clusters of $HSi(OH)_3$ remain on the surface, blocking the corrosion process [72]. However, the applicability of the above model depends on being possible to vary the rate of formation of the poisoning species.

Finally, it is important to mention that related models were also proposed to represent the formation of passive layers at the interface between lithium metal and a solvent [73, 74]. The simplest version of this model is an extension of the Eden model starting from a line of seeds (see Ref. [2], ch. 8). The growth proceeds by incorporation of new particles at any site neighbor to the cluster. These particles may be active or poisoning ones, with probabilities p and $1 - p$. Numerical studies indicate an isotropic percolation transition in this system. This is expected because, contrary to the above models, there is no anisotropy.

VI Concluding remarks

This review discussed various classes of lattice growth models which exhibit depinning transitions, i. e. transitions from a growth phase to a blocked or pinned phase. Most of those transitions are in the directed percolation class, although some important examples fall into other classes. Moreover, depending on the mechanisms of interface growth, different relations are obtained between growth exponents and the exponents of a certain class of dynamical transition. Consequently, those models suggest a large variety of plausible physical situations in which those transitions may be observed, which is certainly a motivation for further theoretical and experimental studies.

Acknowledgements

The author thanks Sergio Botelho, Dante Franceschini, Anna Chame, Robin Stinchcombe and Sergio Queiroz for helpful discussions, suggestions and collaboration in scientific work during the last years.

This work was partially supported by CNPq and FAPERJ (Brazilian agencies).

References

[1] *Frontiers in Surface and Interface Science*, edited by Charles B. Duke and E. Ward Plummer (Elsevier, Amsterdam, 2002).

[2] A.-L. Barabási and H. E. Stanley, *Fractal Concepts in Surface Growth* (Cambridge University Press, New York, 1995).

[3] J. Krug, Adv. Phys. **46**, 139 (1997).

[4] H. Hinrichsen, Adv. Phys. **49**, 815 (2000).

[5] H. Hinrichsen, Braz. J. Phys. **30**, 69 (2000).

[6] H. Ji and M. O. Robbins, Phys. Rev. A **44**, 2538 (1991).

[7] S. V. Buldyrev, A.-L. Barabási, F. Caserta, S. Havlin, H. E. Stanley and T. Vicsek, Phys. Rev. A **45**, R8313 (1992).

[8] L.-H. Tang and H. Leschhorn, Phys. Rev. A **45**, R8309 (1992).

[9] U. Alon, M. R. Evans, H. Hinrichsen, and D. Mukamel, Phys. Rev. Lett. **76**, 2746 (1996).

[10] F. Family, J. Phys. A **19** L441 (1986).

[11] J. M. Kim and J. M. Kosterlitz, Phys. Rev. Lett. **62**, 2289 (1989).

[12] M. J. Vold, J. Coll. Sci. **14** (1959) 168; J. Phys. Chem. **63**, 1608 (1959).

[13] F. Family and T. Vicsek, J. Phys. A **18**, L75 (1985).

[14] M. C. Bartelt and J. W. Evans, Phys. Rev. B **46**, 12675 (1992).

[15] S. Clarke and D. D. Vvedensky, J. Appl. Phys. **63**, 2272 (1988).

[16] C. Ratch, A. Zangwill, P. Smilauer, and D. D. Vvedensky, Phys. Rev. Lett. **72**, 3194 (1994).

[17] S. F. Edwards and D. R. Wilkinson, Proc. R. Soc. London **381**, 17 (1982).

[18] D. Wolf and J. Villain, Europhys. Lett. **13**, 389 (1990).

[19] M. Kardar, G. Parisi and Y.-C. Zhang, Phys. Rev. Lett. **56**, 889 (1986).

[20] B. A. Mello, A. S. Chaves and F. A. Oliveira, Phys. Rev. E **63**, 41113 (2001).

[21] J. Marro and R. Dickman, *Nonequilibrium Phase Transitions in Lattice Models* (Cambridge University Press, Cambridge, 1999).

[22] S. R. Broadbent and J. M. Hammersley, Proc. Camb. Phyl. Soc. **53**, 629 (1957).

[23] J. W. Essam, Rep. Prog. Phys. **43**, 833 (1980).

[24] D. Stauffer and A. Aharony, *Introduction to Percolation Theory*, 2nd. ed. (Taylor & Francis, London/Philadelphia, 1992).

[25] T. E. Harris, Ann. Prob. **2**, 969 (1974).

[26] R. Dickman and J. K. da Silva, Phys. Rev. E **58**, 4266 (1998).

[27] I. Jensen, J. Phys. A **32**, 5233 (1999).

[28] C. A. Voigt and R. M. Ziff, Phys. Rev. E **56**, R6241 (1997).

[29] E. V. Albano, J. Phys. A: Math. Gen. **27**, L881 (1994).

[30] R. M. Ziff, E. Gulari, and Y. Barshad, Phys. Rev. Lett. **56**, 2553 (1986).

[31] H. K. Janssen Z. Phys. B **42**, 151 (1981)

[32] P. Grassberger, Z. Phys. B **47**, 365 (1982).

[33] D. Zhong and D. ben Avraham, Phys. Lett. A **209**, 333 (1995).

[34] I. Jensen, Phys. Rev. E **50**, 3623 (1994).

[35] C. S. Nolle, B. Koiller, N. Martys, and M. O. Robbins, Physica A **205**, 342 (1994).

[36] C. S. Nolle, B. Koiller, N. Martys, and M. O. Robbins, Phys. Rev. Lett. **71**, 2074 (1993).

[37] R. Bruinsma and G. Aeppli, Phys. Rev. Lett. **52**, 1543 (1984).

[38] J. Koplik and H. Levine, Phys. Rev. B **32**, 280 (1985).

[39] D. A. Kessler, H. Levine and Y. Tu, Phys. Rev. A **43**, 4551 (1991).

[40] L.-H. Tang, M. Kardar, and D. Dhar, Phys. Rev. Lett. **74**, 920 (1995).

[41] L. A. N. Amaral, A.-L. Barabási, and H. E. Stanley, Phys. Rev. Lett. **73**, 62 (1994).

[42] M. A. Rubio, C. A. Edwards, A. Dougherty, and J. P. Gollub, Phys. Rev. Lett. **63**, 1685 (1989).

[43] V. K. Horváth, F. Family, and T. Vicsek, J. Phys. A: Math. Gen. **24**, L25 (1991).

[44] S. He, G. L. M. K. S. Kahanda, and P.-Z. Wong, Phys. Rev. Lett. **69**, 3731 (1992).

[45] R. Albert, A.-L. Barabási, N. Carle and A. Dougherty, Phys. Rev. Lett. **81**, 2926 (1998).

[46] F. Family, K. C. B. Chan, and J. Amar, in *Surface Disordering: Growth, Roughening and Phase Transitions*, edited by R. Jullien, J. Kertész, P. Meakin and D. E. Wolf (Nova Science, New York, 1992).

[47] S. V. Buldyrev, A.-L. Barabási, S. Havlin, J. Kertész, H. E. Stanley and H. S. Xenias, Physica A **191**, 220 (1992).

[48] N. Neshkov, Phys. Rev. E **61**, 6023 (2000).

[49] J. J. Ramasco, J. M. López and M. A. Rodríguez, Phys. Rev. E **64**, 66109 (2001).

[50] P. Le Doussal and K. J. Wiese, Phys. Rev. E **67**, 16121 (2003).

[51] U. Alon, M. R. Evans, H. Hinrichsen, and D. Mukamel, Phys. Rev. E **57**, 4997 (1998).

[52] H. Hinrichsen, Phys. Rev. E **67**, 16110 (2003).

[53] U. C. Täuber, M. J. Howard, and H. Hinrichsen, Phys. Rev. Lett. **80**, 2165 (1998).

[54] H. Hinrichsen, R. Livi, D. Mukamel, and A. Politi, Phys. Rev. Lett. **79**, 2710 (1997).

[55] Y. Tu, G. Grinstein, and M. A. Muñoz, Phys. Rev. Lett. **78**, 274 (1997).

[56] M. A. Muñoz and T. Hwa, Europhys. Lett. **41**, 147 (1998).

[57] H. Hinrichsen, R. Livi, D. Mukamel, and A. Politi, Phys. Rev. E **61**, R1032 (2000).

[58] H. Hinrichsen and G. Ódor, Phys. Rev. Lett. **82**, 1205 (1999).

[59] W. Wang and H. A. Cerdeira, Phys. Rev. E **47**, 3357 (1993).

[60] H. F. El-Nashar and H. A. Cerdeira, Phys. Rev. E **60** 1262 (1999).

[61] H. F. El-Nashar and H. A. Cerdeira, Phys. Rev. E **61** 6149 (2000).

[62] S. S. Botelho and F. D. A. Aarão Reis, Phys. Rev. E **65**, 32101 (2002).

[63] F. D. A. Aarão Reis, Phys. Rev. E **66**, 27101 (2002).

[64] J. A. de Sales, M. L. Martins and J. G. Moreira, J. Phys. A: Math. Gen. **32**, 885 (1999).

[65] J. M. Lopez, Phys. Rev. Lett. **83**, 4594 (1999).

[66] M.N. Barber, in *Phase Transitions and Critical Phenomena* Vol. 8, edited by C. Domb and J.L. Lebowitz (Academic, New York, 1983).

[67] M. E. Fisher, in *Critical Phenomena*, Proceedings of the International School of Physics "Enrico Fermi", Course LI, Varenna, 1970, edited by M. S. Green (Academic, New York, 1971).

[68] C. Li, J. E. Quinones, and S. Banerjee, J. Vac. Sci. Technol. A **14**, 170 (1996).

[69] F. Gao, D. D. Huang, J. P. Li, Y. X. Lin, M. Y. Kong, D. Z. Sun, J. M. Li, and L. Y. Lin, J. Crystal Growth **220**, 461 (2000).

[70] J. H. Edgar, Z. Y. Xie and D. N. Braski, Diamond Relat. Mater. **7**, 35 (1998).

[71] F. D. A. Aarão Reis, to appear in Phys. Rev. E (2003).

[72] M. E. R. Dotto and M. U. Kleinke, Phys. Rev. B **65**, 245323 (2002).

[73] I. Nainville, A. Lemarchand, and J.-P. Badiali, Phys. Rev. E **53**, 2537 (1996).

[74] M. Lafage, V. Russier, and J. P. Badiali, J. Electroanal. Chem. **450**, 203 (1998).